Soft Science

Mechanically flexible and flame-retardant cellulose nanofibril-based films integrated with MXene and chitosan

Shi-Neng Li[1,#,*], Zi-Fan Zeng[1,#], Xiao-Feng He[1], Zhi-Chao Xu[1], Yu-Hang Luo[1], Qing-Yue Ni[1], Li Peng[2,*], Li-Xiu Gong[3], Yang Li[4], Baiyu Jiang[1,*]

[1]College of Chemistry and Materials Engineering, Zhejiang A & F University, Hangzhou 311300, Zhejiang, China.

[2]ZJU-Hangzhou Global Scientific and Technological Innovation Center, School of Micro-Nano Electronics, Zhejiang University, Hangzhou 310027, Zhejiang, China.

[3]Key Laboratory of Organosilicon Chemistry and Material Technology of Ministry of Education, College of Material, Chemistry and Chemical Engineering, Hangzhou Normal University, Hangzhou 311121, Zhejiang, China.

[4]Department of Nano-physics, Gachon University, Seongnam-si, Gyeonggi-do 13120, Korea.

[#]Authors contributed equally.

Correspondence to: Dr. Shi-Neng Li, College of Chemistry and Materials Engineering, Zhejiang A & F University, 666 Wusu Street, Lin'an District, Hangzhou 311300, Zhejiang, China. E-mail: lisn@zafu.edu.cn; Prof. Li Peng, MOE Key Laboratory of Macromolecular Synthesis and Functionalization, Department of Polymer Science and Engineering, Zhejiang University, 733 Jianshesan Road, Xiaoshan District, Hangzhou 310027, Zhejiang, China. E-mail: l-peng@zju.edu.cn; Dr. Baiyu Jiang, College of Chemistry and Materials Engineering, Zhejiang A & F University, 666 Wusu Street, Lin'an District, Hangzhou, 311300, Zhejiang, China. E-mail: jiangby@zafu.edu.cn

Supplementary Figures

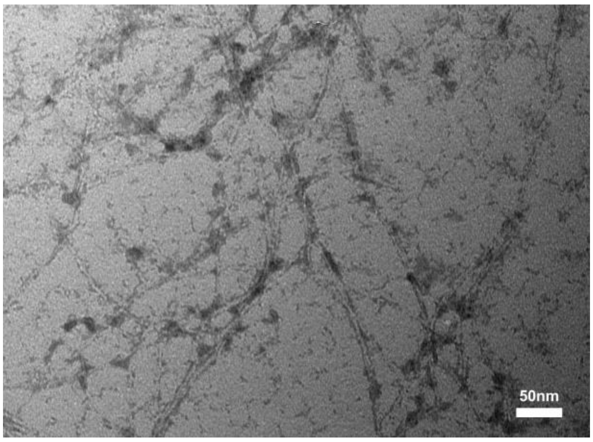

Figure. S1 TEM image of PCNF.

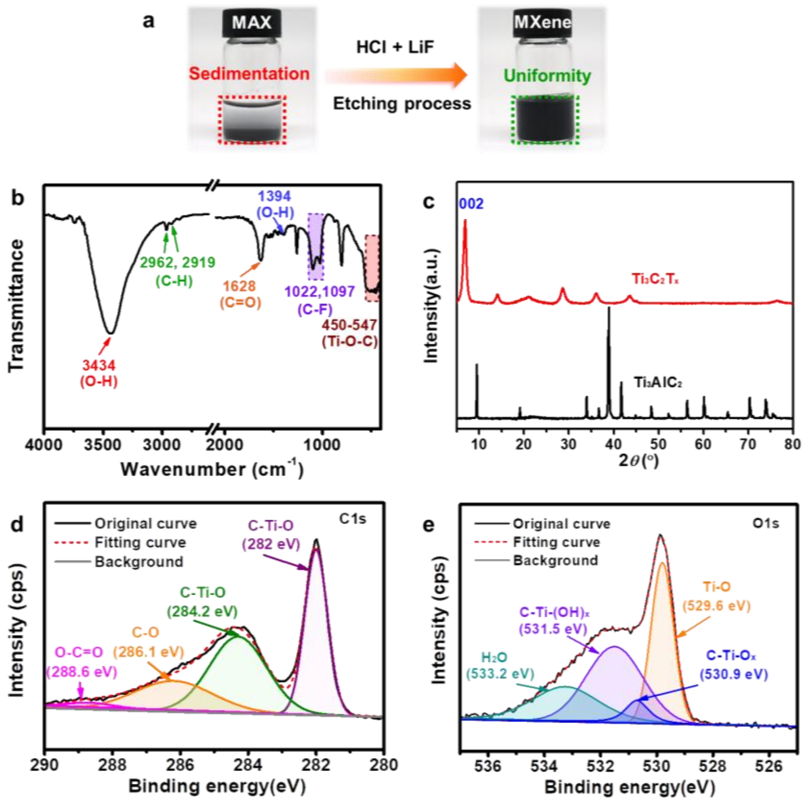

Figure. S2 (a) Digital photos of the fabrication process of MXene nanosheets. A dark green and uniform suspension can be achieved when MAX is treated by acid etching method. Characterization of chemical structure: (b) FT-IR, (c) XRD, (d) C1s and (e) O1s spectra.

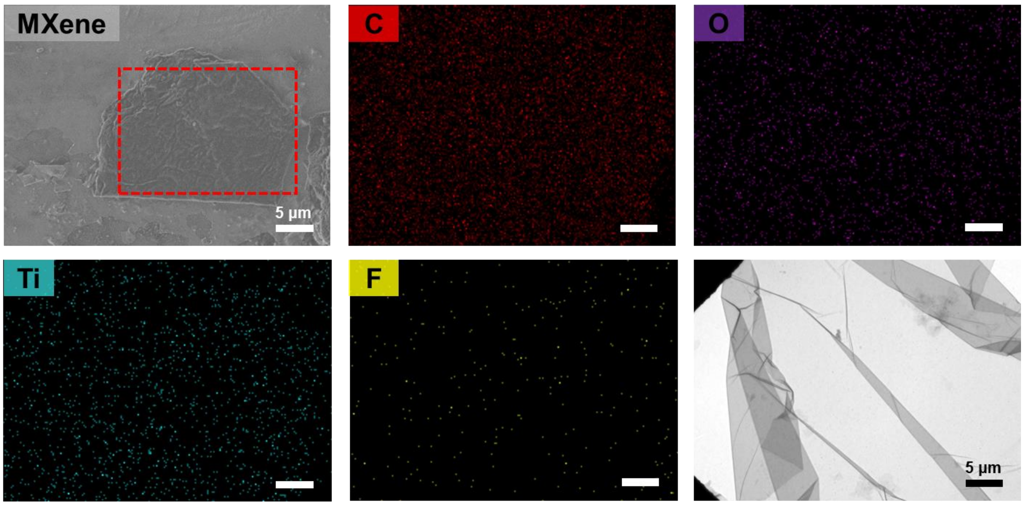

Figure. S3 SEM image and corresponding element mapping of MXene nanosheets.

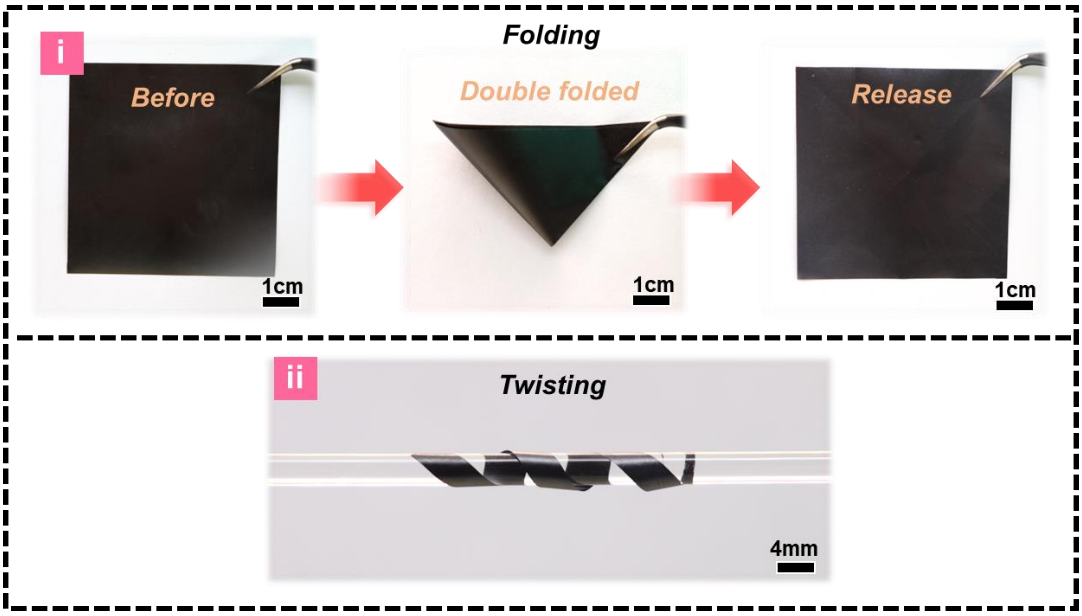

Figure. S4 Digital photographs of PCNF/CS-M film, the excellent mechanical strength and flexibility can make it withstand (i) folding and (ii) twisting, and no cracks or damages are observed.

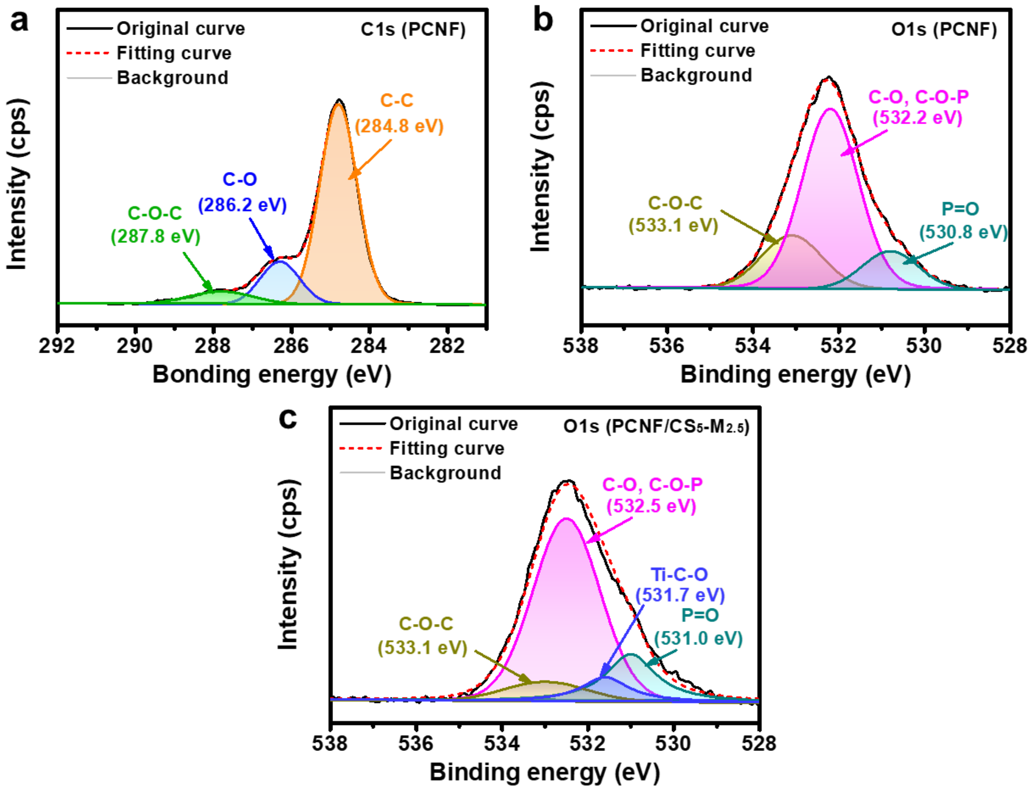

Figure. S5 (a) C1s and (b) O1s XPS spectra of PCNF and (c) O1s XPS spectrum of PCNF/CS_{15}-$M_{5.0}$.

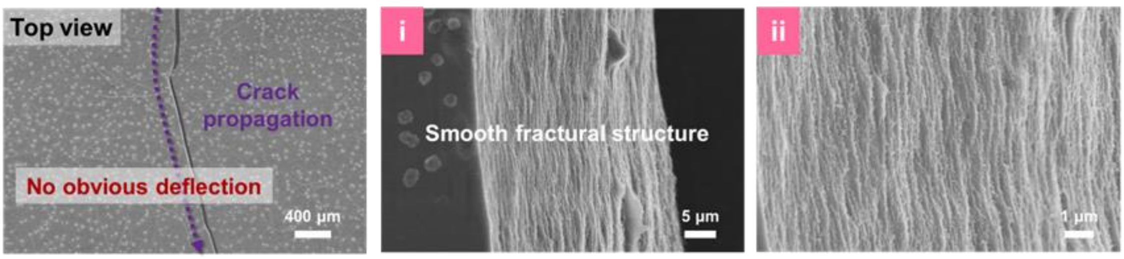

Figure. S6 SEM images of PCNF film after simple stretching.

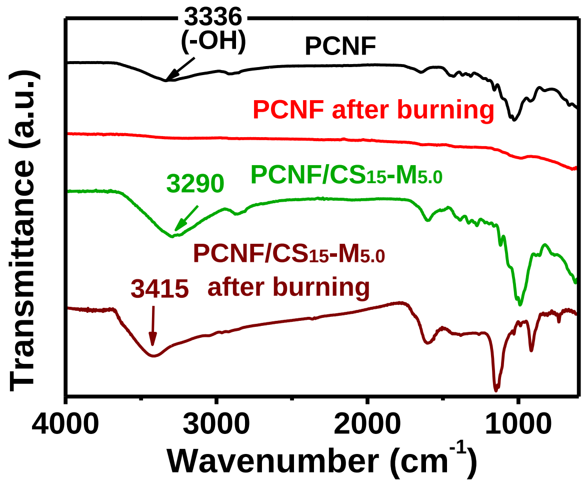

Figure. S7 FT-IR spectra of PCNF and PCNF/CS_{15}-$M_{5.0}$ films before and after burning.

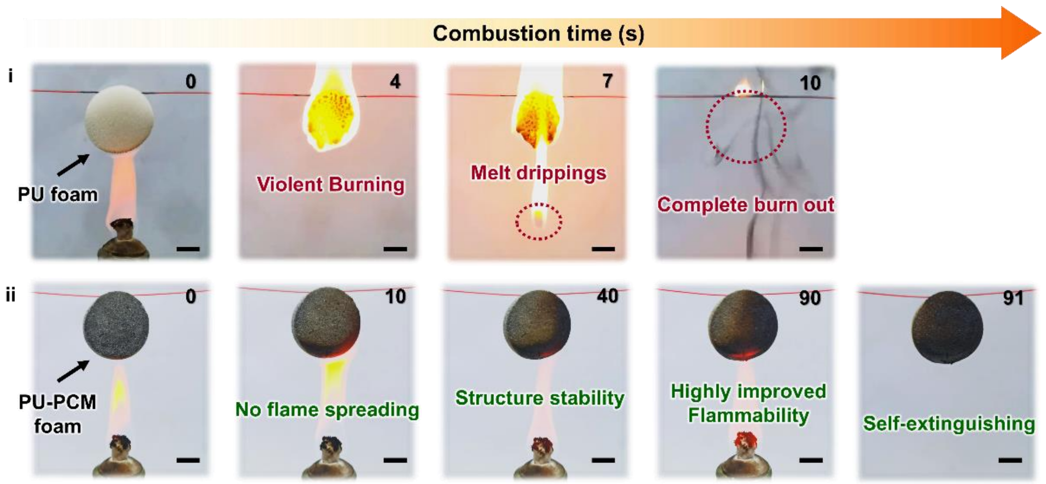

Figure. S8 Flame burning tests for various PU composites: (i) pure PU foam and (ii) PCM-PU foam. Scale bars are 1cm.

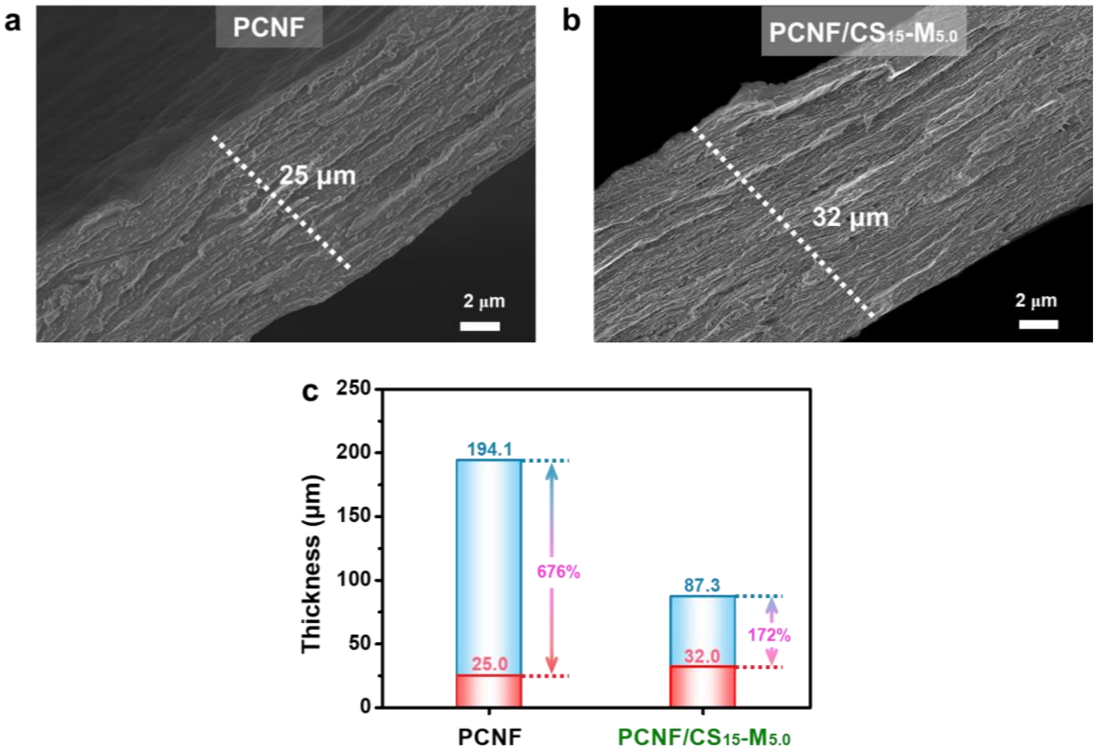

Figure. S9 SEM images of (a) PCNF and (b) PCNF/CS_{15}-$M_{5.0}$ films; (c) Thickness change of PCNF and PCNF/CS_{15}-$M_{5.0}$ paper after combustion.

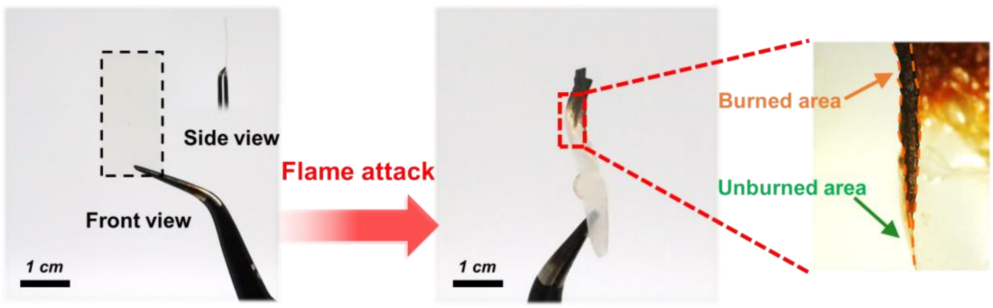

Figure. S10 Digital photographs of the PCNF film before/after being exposed to the butane flame.

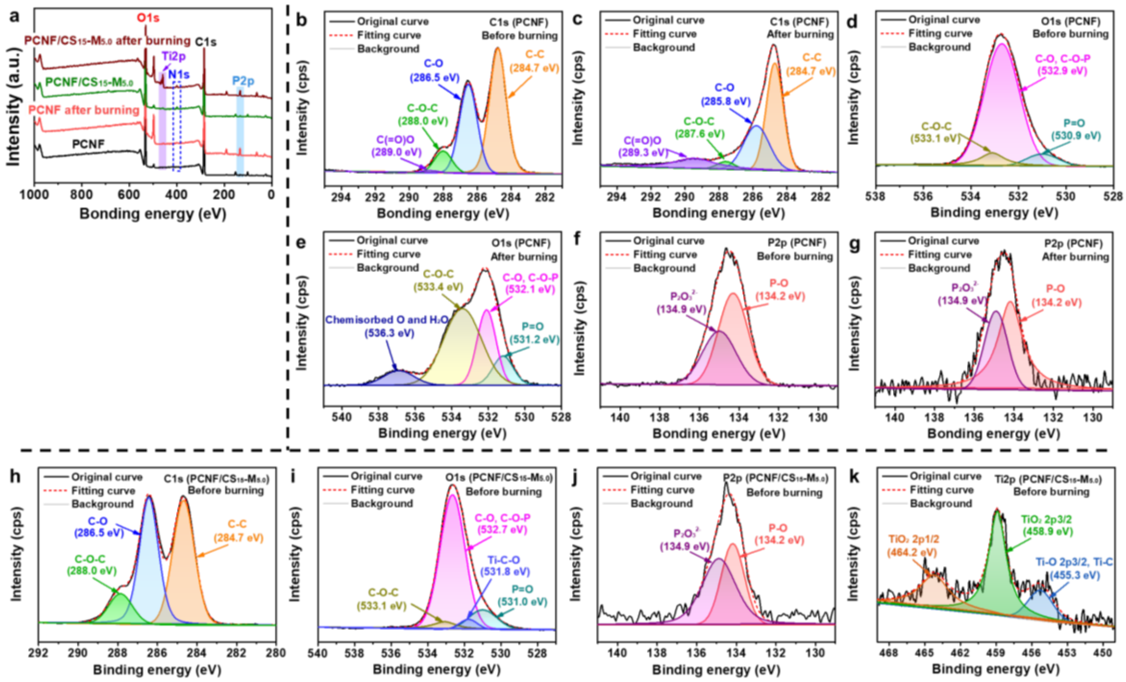

Figure. S11 (a) Full-scan XPS spectra of PCNF and PCNF/CS_{15}-$M_{5.0}$ before and after burning; C1s XPS spectrum of PCNF before (b) and after (c) burning; O1s XPS spectrum of PCNF before (d) and after (e) burning; P2p XPS spectrum of PCNF before (f) and after (g) burning; (h) C1s, (i) O1s, (j) P2p and (k) Ti2p XPS spectra of PCNF/ CS_{15}-$M_{5.0}$ before burning.

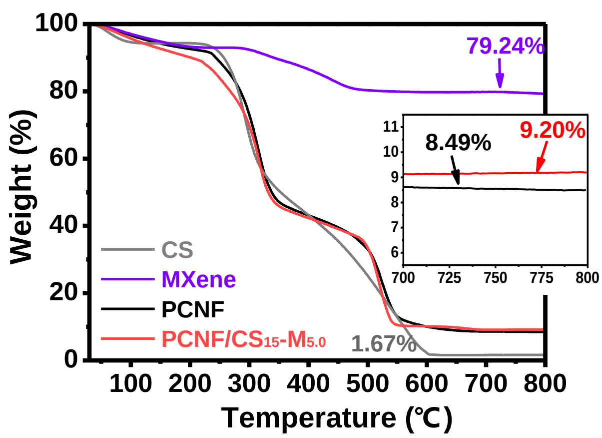

Figure. S12 TGA curves of CS, MXene, PCNF and PCNF/CS_{15}-$M_{5.0}$ film.

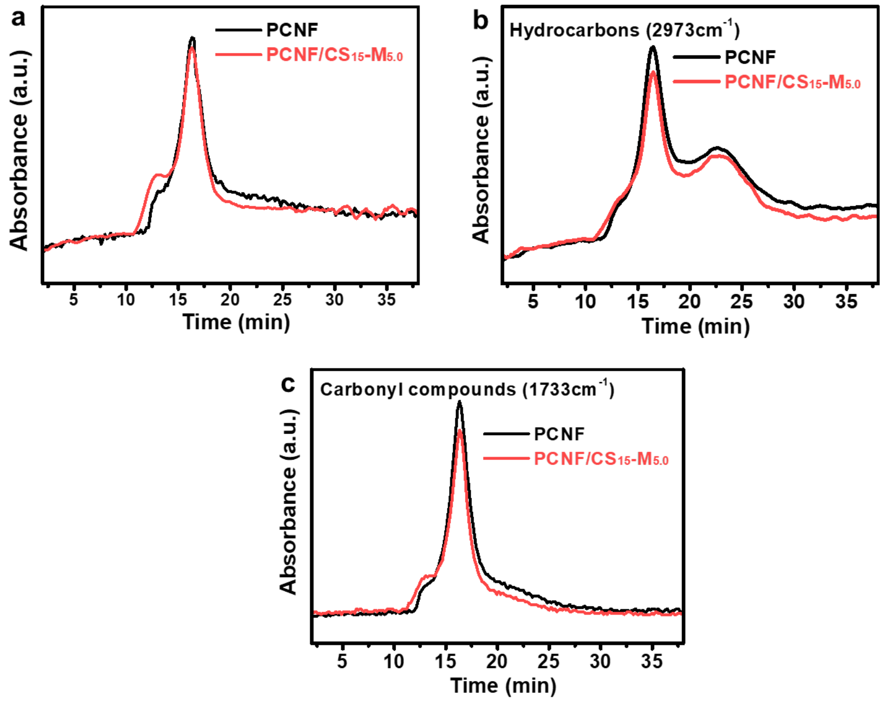

Figure. S13 (a) Total absorptions spectra of the gaseous products for PCNF and PCNF/CS_{15}-$M_{5.0}$; The pyrolysis products of the PCNF and PCNF/CS_{15}-$M_{5.0}$ at the maximum decomposition rate: (b) hydrocarbons and (c) carbonyl compounds.

Supplementary Tables

Table S1. Recipes of precursor solutions for the synthesis of PCNF/CS-M paper.

Sample	PCNF (g)	CS (wt%)	MXene (wt%)	H_2O (mL)
PCNF	0.2	0	0	50
PCNF/CS_5	0.2	5	0	50
PCNF/CS_{10}	0.2	10	0	50
PCNF/CS_{15}	0.2	15	0	50
PCNF/CS_{20}	0.2	20	0	50
PCNF/$M_{2.5}$	0.2	0	2.5	50
PCNF/CS_5-$M_{2.5}$	0.2	5	2.5	50

PCNF/CS_{15}-$M_{2.5}$	0.2	15	2.5	50
PCNF/CS_{15}-$M_{5.0}$	0.2	15	5.0	50
PCNF/CS_{15}-$M_{7.5}$	0.2	15	7.5	50
PCNF/CS_{15}-$M_{10.0}$	0.2	15	10.0	50

Table S2. Tensile properties of various nanocomposite films.

Sample	Tensile strength (MPa)	Tensile strain (%)	Toughness (MJ m^{-3})	Young's modulus (GPa)
PCNF	61.6 ±4.1	30.5 ±2.9	12.7 ±1.1	0.82 ±0.04
PCNF/CS_5	72.1 ±4.9	27.1 ±2.5	14.8 ±0.8	1.11 ±0.05
PCNF/$M_{2.5}$	93.6 ±8.2	15.0 ±1.1	8.6 ±0.5	1.16 ±0.05
PCNF/CS_5-$M_{2.5}$	135.3 ±9.3	22.0 ±0.9	18.9 ±0.6	1.21 ±0.06

Table S3. Tensile properties of PCNF films with variational CS content.

Sample	Tensile strength (MPa)	Tensile strain (%)	Toughness (MJ m^{-3})	Young's modulus (GPa)
PCNF	61.6 ±4.1	30.5 ±2.9	12.7 ±1.1	0.82 ±0.04
PCNF/CS_5	72.1 ±4.9	27.1 ±2.5	14.8 ±0.8	1.11 ±0.05
PCNF/CS_{10}	82.4 ±4.4	17.1 ±1.0	10.3 ±0.4	1.40 ±0.11
PCNF/CS_{15}	134.4 ±8.1	11.2 ±0.7	8.4 ±0.5	1.80 ±0.12
PCNF/CS_{20}	111.0 ±6.7	4.7 ±0.3	3.2 ±0.2	3.00 ±0.22

Table S4. Tensile properties of PCNF/CS_{15}-M films with different MXene content.

Sample	Tensile strength (MPa)	Tensile strain (%)	Toughness (MJ m^{-3})	Young's modulus (GPa)
PCNF/CS_{15}	134.4 ±8.1	11.2 ±0.7	8.4 ±0.5	1.8 ±0.1

PCNF/CS_{15}-$M_{2.5}$	150.1 ±8.3	9.1 ±0.5	8.2 ±0.5	2.7 ±0.2
PCNF/CS_{15}-$M_{5.0}$	172.1 ±9.6	8.0 ±0.5	8.5 ±0.5	4.4 ±0.2
PCNF/CS_{15}-$M_{7.5}$	134.3 ±7.5	4.5 ±0.3	4.2 ±0.2	7.4 ±0.4
PCNF/CS_{15}-$M_{10.0}$	113.8 ±6.3	1.6 ±0.1	1.3 ±0.1	15.4 ±0.9

Table S5. Comparisons of mechanical properties of flame-retardant films

Composition	*Tensile strength (MPa)*	*Tensile strain (%)*	*Toughness （$MJ{\cdot}m^{-3}$）*	*Reference*
AX-BG	14.4	5.7	~0.5	[1]
PEG-MMT-GONR	14.8	3.1	~0.2	[2]
PEI-GO	52.7	4.0	~1.3	[3]
BPI-COOAl	63.7	11.0	~4.2	[4]
PBI-(PWA-IL)	75.5	13.2	~7.9	[5]
HCPA-GO	94.7	2.2	1.4	[6]
f-SiO_2-GO	122.4	6.9	4.7	[7]
WH-MMT-GO	124.0	4.7	~3.6	[8]
PCNF-TA-GO	132.2	1.2	~0.9	[9]
PhC	150.0	7.5	8.2	[10]
GM-BNT-GO	231.1	3.3	4.5	[11]
HCCP-GO	240.0	4.4	~6.1	[12]
PCNF/CS-M	***172.1***	***8.0***	***8.5***	***This work***

AX: Arabinoxylans; **BG:** β-glucan; **PEG:** polyethylene glycol; **MMT:** montmorillonite; **GONR:** graphene oxide nanoribbon; **PEI:** Polyetherimide; **GO:** graphene oxide; **BPI-COOAl:** biopolyimide salt with aluminum; **PBI:** polybenzimidazole; **PWA-IL:** 1-butyl-3-methyl imidazolium phosphotungstate; **HCPA:** amino-modified hexachlorophosphazene; **f-SiO_2:** functionalized silica; **WH:** Wood auto-hydrolysates; **PCNF:** phosphorylated-cellulose nanofibrils; **TA:** tannic acid **PhC:** phosphorylated cellulose; **GM:** galactomannan; **BNT:** bentonite; **HCCP:** hexachlorocyclotriphosphazene; **CS:** chitosan; **M:** MXene

Table S6. TGA data of raw materials and composite films in air atmosphere.

Sample	$T_{5\%}$ (^{o}C)	$T_{10\%}$ (^{o}C)	T_{max} (^{o}C)	Ash800^{o}C (wt%)
CS	89.3	256.4	294.2	1.7
MXene	144.4	341.4	437.8	79.2
PCNF	129.9	242.9	314.8	8.5
PCNF/CS_{15}-$M_{5.0}$	109.4	201.5	317.4	9.2

Table S7. Characteristic parameters of PCNF and PCNF/CS_{15}-$M_{5.0}$ from MCC.

Sample	HRC (J/g□K)	PHRR (W/g)	THR (kJ/g)	T_{PHRR} (^{o}C)
PCNF	93.0	95.2	6.7	325.8
PCNF/CS_{15}-$M_{5.0}$	70.0	70.8	5.3	329.2

REFERENCES

[1] Ali U, Bijalwan V, Basu S, Kesarwani AK, Mazumder K. Effect of beta-glucan-fatty acid esters on microstructure and physical properties of wheat straw arabinoxylan films. Carbohydr Polym 2017;161: 90-98. [DOI: 10.1016/j.carbpol.2016.12.036]

[2] Yu Z.-R., Mao M., Li S.-N. et al. Facile and green synthesis of mechanically flexible and flame-retardant clay/graphene oxide nanoribbon interconnected networks for fire safety and prevention. Chem Eng J 2021;405: 126620. [DOI: 10.1016/j.cej.2020.126620]

[3] Lopez V, Paton-Carrero A, Romero A, Valverde JL, Sanchez-Silva L. Improvement of the mechanical and flame-retardant properties of polyetherimide membranes modified with Graphene oxide. Polym-Plast Tech Mat 2018;58: 1170-1177. [DOI: 10.1080/03602559.2018.1542723]

[4] Phanthuwongpakdee J, Harimoto T, S Babel, Dwivedi S, Takada K, Kaneko T. Flame retardant transparent films of thermostable biopolyimide metal hybrids, Polym Degrad Stab 2021;188: 109571. [DOI: 10.1016/j.polymdegradstab.2021.109571]

[5] Li J, Wang S, Liu F et al. Flame-retardant AEMs based on organic-inorganic

composite polybenzimidazole membranes with enhanced hydroxide conductivity. J Membr Sci 2019;591: 117306. [DOI: 10.1016/j.memsci.2019.117306]

[6] Cao CF, Yu B, Chen ZY et al. Fire intumescent, high-temperature resistant, mechanically flexible graphene oxide network for exceptional fire shielding and ultra-fast fire warning. Nano-Micro Lett 2022;14(1) : 92. [DOI: 10.1007/s40820□022□00837□1]

[7] Yu Z-R, Li S-N, Zang J et al. Enhanced mechanical property and flame resistance of graphene oxide nanocomposite paper modified with functionalized silica nanoparticles. Compos Part B-Eng 2019;177: 107347. [DOI: 10.1016/j.compositesb.2019.107347]

[8] Chen G-G, Hu Y-J, Peng F et al. Fabrication of strong nanocomposite films with renewable forestry waste/montmorillonite/reduction of graphene oxide for fire retardant. Chem Eng J 2018;337: 436-445. [DOI: 10.1016/j.cej.2017.12.119]

[9] Cao C-F, Yu B, Guo B-F et al. Bio-inspired, sustainable and mechanically robust graphene oxide-based hybrid networks for efficient fire protection and warning. Chem Eng J 2022;439: 134516. [DOI: 10.1016/j.cej.2022.134516]

[10] Hou G, Zhao S, Li Y, Fang Z, Isogai A. Mechanically robust, flame-retardant phosphorylated cellulose films with tunable optical properties for light management in LEDs. Carbohydr Polym 2022;298: 120129. [DOI: 10.1016/j.carbpol.2022.120129]

[11] Tao Y, Huang C, Lai C, Huang C, Yong Q. Biomimetic galactomannan/bentonite/graphene oxide film with superior mechanical and fire retardant properties by borate cross-linking. Carbohydr Polym 2020;245: 116508. [DOI: 10.1016/j.carbpol.2020.116508]

[12] Dong L, Hu C, Song L, Huang X, Chen N, Qu L. A large-area, flexible, and flame-retardant graphene paper. Adv Funct Mater 2016;26: 1470-1476. [DOI: 10.1002/adfm.201504470]